# Interaction of an Antituberculosis Drug with a Nanoscopic Macromolecular Assembly: Temperature-Dependent Förster Resonance Energy Transfer Studies on Rifampicin in an Anionic Sodium Dodecyl Sulfate Micelle

Tanumoy Mondol,[†] Priya Rajdev,[†] Abhinandan Makhal,[†] and Samir Kumar Pal*,[†]

Unit for Nano Science & Technology, Department of Chemical, Biological, and Macromolecular Sciences, S. N. Bose National Centre for Basic Sciences, Block JD, Sector III, Salt Lake, Kolkata 700 098, India

ABSTRACT: In this contribution, we report studies on the nature of binding of a potent antituberculosis drug, Rifampicin (RF) with a model drug delivery system, sodium dodecyl sulfate (SDS) micelle. Temperature dependent dynamic light scattering (DLS), conductometry, and circular dichroism (CD) spectroscopy have been employed to study the binding interaction of the drug with the micelle. The absorption spectrum of the drug RF in the visible region has been employed to study Förster resonance energy transfer (FRET) from another fluorescent drug Hoechst 33258 (H33258), bound to the micelle. Picosecond-resolved FRET studies at room temperature confirm the simultaneous binding of the two drugs to the micelle and the distance between the donor–acceptor pair is found to be 34 Å. The temperature dependent FRET study also confirms that the location and efficiency of drug binding to the micelle changes significantly at the elevated temperature. The energy transfer efficiency of the donor H33258, as measured from time-resolved studies, decreases significantly from 76% at 20 °C to 60% at 55 °C. This reveals detachment of some amount of the drug molecules from the micelles and increased donor–acceptor distance at elevated temperatures. The estimated donor–acceptor distance increases from a value of 33 Å at 20 °C to 37 Å at 55 °C. The picosecond resolved FRET studies on a synthesized DNA bound H33258 in RF solution have been performed to explore the interaction between the two. Our studies are expected to find relevance in the exploration of a potential vehicle for the vital drug rifampicin.
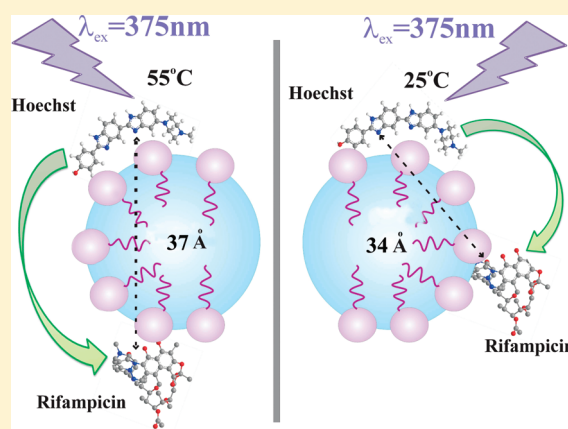
■ INTRODUCTION

Characterization of a drug molecule becomes extremely important when it is related with one of the detrimental diseases and very few of such drugs are available for the management of such diseases. Tuberculosis (TB) is an example of such disease for which limited number of antibiotics, for example, Rifampicin, Isoniazid, and Ethambutol, are the essential choices for the clinical disease management.[1−7] Among others, Rifampicin (RF) is a potent antituberculosis drug and has enormous pharmacological significance. It is a very effective antibiotic, particularly active against *Mycobacterium tuberculosis*, *M. bovis*, *M. avium* complex, and *M. intracellulare*,[8−12] and hence it is highly effective in the treatment of TB. It is known that RF is a specific inhibitor of bacterial RNA polymerase, which acts by direct interaction with the enzyme,[13] probably by inhibiting the process of transcription at the level of initiation.[14−16] Although, RF is poorly soluble in aqueous media,[17] it is a clinically effective drug. The inescapable necessity and poor solubility of RF automatically necessitates an alternate drug delivery/carrier system.[17−21] In this regard, the interaction of RF with various potential drug carrier systems is essential. However, such studies on the

encapsulation of the drug in other macromolecules/molecular assemblies in present literature are sparse. One of the early conductometry studies investigated the interaction of the drug with β-cyclodextrin, a potential drug delivery system.[22] It is well-known that macromolecular assemblies like micelles are also very efficient drug delivery system for the solubilization of hydrophobic drugs.[23,24] However, until date no study has been initiated on the interaction of the vital drug RF with micelles. Exploration of the binding interaction of the anti-TB drug, RF with a model micelle (sodium dodecyl sulfate; SDS) is the motive of the present work. Although, the drug RF has very distinct spectroscopic signature including optical absorption and circular dichroism (CD), the spectroscopic properties have not been used in earlier studies to investigate the interaction of the drug with other macromolecular assembly.

Here, dynamic light scattering (DLS) and conductometric techniques have been used to investigate the integrity of the

nanoscopic macromolecular assembly of SDS micelle upon binding of the drug RF. We have also used CD spectroscopy to explore the binding interaction of the drug with the SDS micelle and also to investigate the thermal stability of the drug-micelle complex. The optical absorption spectrum of the drug RF in the visible region has been exploited for the dipolar interaction with another, micelle-bound fluorescent antihelmenthic drug, Hoechst 33258 (H33258). Here time-correlated single photon counting (TCSPC) spectroscopy has been utilized to investigate the coexistence of the drug with H33258 and also to locate the binding of the same with respect to H33258, bound to the macromolecular SDS micellar assembly. Temperature-dependent Förster resonance energy transfer (FRET) studies from the donor H33258 to the acceptor RF at the micellar surface confirm the physical attachment of the drug RF to the SDS micelle and the thermal stability of the simultaneous drug binding capability of the host micelle. We have also used FRET to study the interaction of the drug RF with a synthesized dodecamer DNA. The studies are expected to find its relevance in the exploration of alternate drug delivery systems for the poorly aqueous soluble drug like RF.

■ MATERIALS AND METHODS

Hoechst 33258 (H33258) was purchased from Molecular probes. Rifampicin, sodium dihydrogen phosphate, and disodium hydrogen phosphate (for the preparation of phosphate buffer) were purchased from Sigma. Sodium dodecyl sulfate (SDS) was purchased from Fluka and used without any further purification. Dodecamer (5'CGCGAATTCGCG3') DNA was purchased from Trilink (USA). A 100 mM phosphate buffer (pH 7) was prepared by using sodium dihydrogen phosphate (50 mM), disodium hydrogen phosphate (50 mM) in Millipore water and the sample solutions were prepared in the same.

The DLS measurements were done in a Nano S Malvern-instrument employing a 4 mW He−Ne laser (λ = 632.8 nm) equipped with a thermostatic sample chamber. All the scattered photons were collected at 173° scattering angle. The scattering intensity data were processed using the instrumental software to obtain the hydrodynamic diameter (d_H) and the size distribution of the scatterer in each sample. The instrument measures the time dependent fluctuation in the intensity of light scattered from the particles in solution at a fixed scattering angle. Hydrodynamic diameter of the clusters was estimated from the intensity auto-correlation function of the time-dependent fluctuation in intensity. Hydrodynamic diameter is defined as $d_H = (k_b T)/(3\pi\eta D)$ where, k_b is the Boltzmann constant, η is the solvent (here, water) viscosity, and D is the translational diffusion coefficient. The resolution of the instrument is 0.6 nm.

The conductivity of mixtures was measured with two platinum electrodes and digital conductivity bridge, Sensino 378 conductivity meter. Measurement of conductivity was carried out with an absolute accuracy up to ±0.5%. An accuracy of ±0.3 °C was assured in the temperature-dependent experiments. The conductivity measurements were done at different temperatures for SDS/buffer binary system and for SDS/RF/buffer ternary system, as a function of SDS concentration keeping RF concentration constant at 2×10^{-4} M. CD measurements were carried out on a JASCO 815 spectro-polarimeter with a temperature controller attachment. The scan speed of the measurements was 50 nm/min and each spectrum was the average of five scans. Buffer solutions containing the corresponding concentration of

the surfactant, that is, SDS, were subtracted from all the measurements. The concentration of the drug RF was 43 × 10^{-6} M, and the SDS concentration was varied from 1×10^{-3} to 50×10^{-3} M. The results were expressed in θ, the optical rotation obtained from the instrument in millidegrees and also as molar ellipticity $[\theta]$ in M·cm·mdegrees^{-1}. The temperature dependent CD experiments were done on taking 11×10^{-6} M RF and SDS of concentration 8×10^{-3} and 20×10^{-3} M. All absorbance measurements were performed in a Shimadzu UV-2450 spectrophotometer and fluorescence measurements were performed in a Jobin Yvon Fluoromax-3 fluorimeter. For the steady state fluorescence experiments, 11.47×10^{-6} M H33258 and 20.13×10^{-3} M SDS were used and RF concentration was maintained at 1×10^{-4} M.

The details of the picosecond-resolved spectroscopic data (including transients and time-resolved anisotropy) were measured with commercially available time correlated single photon counting (TCSPC) setup from Edinburgh Instruments (instrument response function, IRF = 60 ps), in which the sample was excited at 375 nm. The picosecond-resolved fluorescence transients have been fitted with triexponential function, $\sum_{i=1}^{3} A_i \exp(-t/\tau_i)$, where, A_i's are weight percentages of the decay components with time constants of τ_i. The relative change in the overall excited state lifetime is expressed by the equation $\tau = \sum_{i=1}^{3} A_i \tau_i$, when $\sum_{i=1}^{3} A_i = 1$. For the energy transfer experiments,[25] the concentration of H33258 was 11.47×10^{-6} M whereas, for RF and SDS, it was 182×10^{-6} and 20×10^{-3} M respectively. We have used 8×10^{-6} M of H33258, 10×10^{-6} M DNA, and 50×10^{-6} M RF to investigate the possibility of binding of RF to DNA. The Förster resonance energy transfer distances of donor−acceptor pairs were calculated using the equation[25]

$$R_0 = 0.211[\kappa^2 n^{-4} Q_D J(\lambda)]^{1/6} (\text{In Å}) \tag{1}$$

where R_0 is the distance between the donor and the acceptor at which the energy transfer efficiency is 50%, and κ^2 is a factor describing the relative orientation of the transition dipoles of the donor and acceptor in space. The acceptor RF can bind to the micelle at any orientation with respect to the donor H33258. Thus for an ensemble of donor−acceptor (D−A) pairs the relative orientation of the D−A is not supposed to be constant and the magnitude of κ^2 is assumed to be two-thirds for donor and acceptors. The refractive index (n) of the medium was assumed to be 1.4 (aqueous medium). Q_D, the quantum yields of the donor in the absence of acceptor were reported for H33258-micelle and H33258-DNA to be 0.54 and 0.53, respectively.[26] $J(\lambda)$, the overlap integral, which expresses the degree of spectral overlap between the donor emission and the acceptor absorption, is given by

$$J(\lambda) = \frac{\int_0^\infty F_D(\lambda)\varepsilon_A(\lambda)\lambda^4 \, d\lambda}{\int_0^\infty F_D(\lambda)d\lambda} \tag{2}$$

where $F_D(\lambda)$ is the fluorescence intensity of the donor in the wavelength range of λ to $\lambda + d\lambda$ and is dimensionless. $\varepsilon_A(\lambda)$ is the extinction coefficient (in $M^{-1} cm^{-1}$) of the acceptor at λ. If λ is in nanometers, then $J(\lambda)$ is in units of $M^{-1} cm^{-1} nm^4$. Once the value of R_0 is known, the donor−acceptor distance (r_{DA}) can easily be calculated using the formula

$$r_{DA}^6 = \frac{[R_0^6(1-E)]}{E} \tag{3}$$

2925

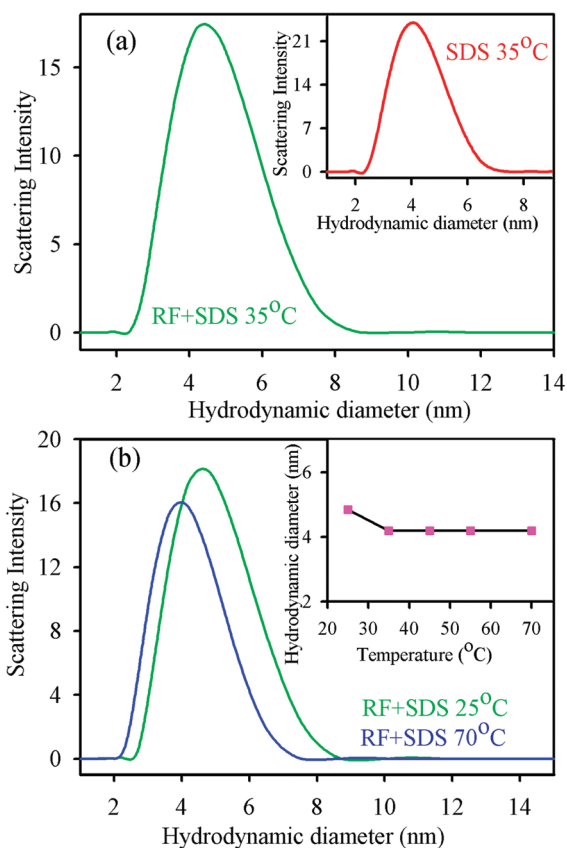dx.doi.org/10.1021/jp108115h |J. Phys. Chem. B 2011, 115, 2924–2930

Figure 1. (a) Scattering intensity of 50 mM SDS micelle−RF (RF + SDS) complex as obtained from the DLS study. A typical DLS signal of SDS micelles without RF at 35 °C has been depicted in the inset. (b) Scattering intensity of 50 mM SDS micelle−RF complex at temperatures 25 and 70 °C. Inset shows the hydrodynamic diameters of the SDS micelle−RF complex at different temperatures.

Here, E is the efficiency of energy transfer. The transfer efficiency can be measured using the relative fluorescence intensity of the donor in the absence (F_D) and presence (F_{DA}) of the acceptor (eq 4a). The efficiency, E can also be calculated from the lifetimes $(\tau_D$ and $\tau_{DA})$ using the eq 4b, where τ_D and τ_{DA} are lifetimes of the donor in absence and in presence of the acceptor, respectively.

$$E = 1 - \frac{F_{DA}}{F_D} \qquad (4a)$$

$$E = 1 - \frac{\tau_{DA}}{\tau_D} \qquad (4b)$$

The potential danger of using the eq 4a for the estimation of resonance energy transfer has been discussed earlier.[27] For anisotropy $(r(t))$ measurements, emission polarization was adjusted to be parallel or perpendicular to that of the excitation and anisotropy is defined as

$$r(t) = \frac{[I_{para} - GI_{perp}]}{[I_{para} + 2GI_{perp}]} \qquad (5)$$

where G, the grating factor, is determined following tail matching technique[28] and found out to be nearly 1. The time-resolved anisotropy of a fluorophore/probe reveals the physical motion of the probe in a microenvironment. The time constants reflect
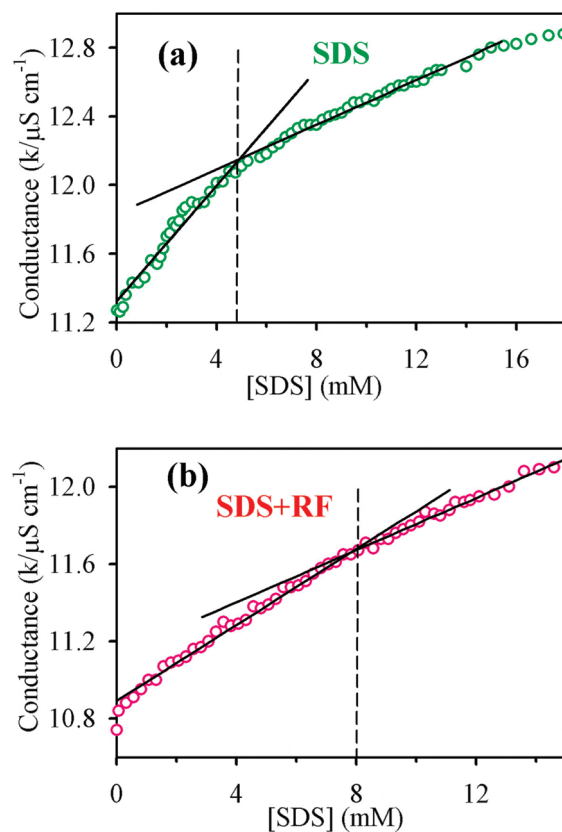

Figure 2. Conductivity (κ) plots. (a) SDS/buffer (SDS) binary system and (b) SDS/RF/buffer (SDS + RF) ternary system with varying [SDS] concentration keeping the RF concentration constant.

rotational correlation time of the probe in the microenvironment.

■ RESULTS AND DISCUSSIONS

As RF is hydrophobic in nature, it can bind to nanoscopic macromolecular assembly of SDS, which is amphiphilic in nature.[29] The sizes of the micelles are determined using the DLS measurements. It is observed that SDS micelles produce spherical and monodispersed droplets, in aqueous buffer, of hydrodynamic diameter (d_H) of ∼4 nm (inset of Figure 1a). As shown in Figure 1a, the hydrodynamic diameter of the micelle remains unaltered upon binding of RF. Given the fact that RF is an amphoteric molecule and at pH 7 it remains in Zwitterionic form[30] interacting with the headgroup of the SDS micelle, the drug is expected to stay at the micelle−water interface.

Figure 1b depicts the stability of RF−SDS micelle complex at various temperatures. The average hydrodynamic diameter of SDS micelle−RF complex at room temperature of 4.85 nm (25 °C) does not change appreciably when temperature is increased up to 70 °C (inset of Figure 1b). Therefore, it indicates that SDS micelle−RF complex maintains its nanoscopic assembly even at higher temperature. However, a change in the scattering intensity is observed with increase in temperature which can be attributed to the increase in the critical micellar concentration (CMC) of the SDS micelle resulting in decrease in the number of SDS micelles at 70 °C.

Figure 2a shows the variation of conductivity of the SDS/buffer binary solution as a function of SDS concentration. It is
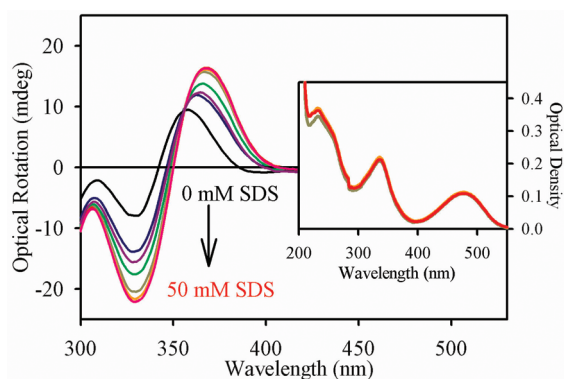
Figure 3. Optical rotation (mdeg) of RF with increasing concentration of SDS (0−50 mM). The inset shows the optical density of RF with increasing concentration of SDS.
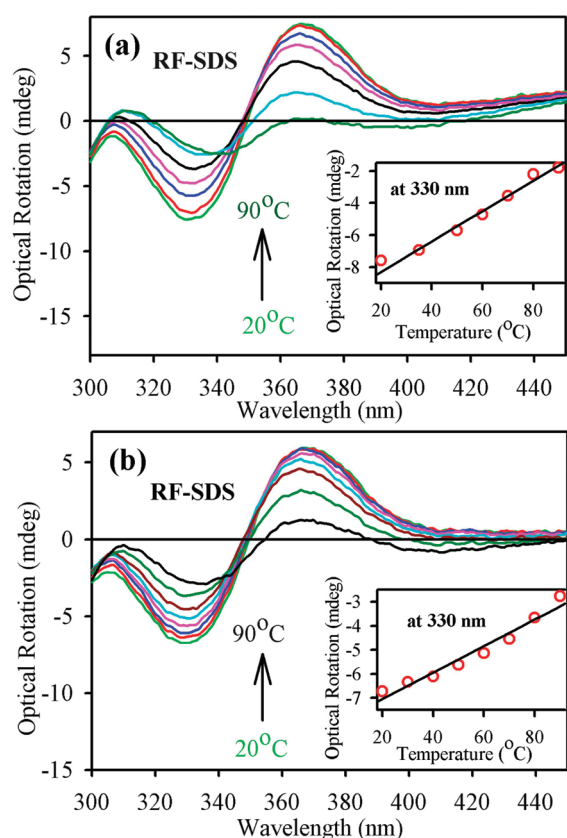

Figure 4. (a) Optical rotation (mdeg) of 8×10^{-3} M SDS−RF complex with increasing temperatures. Inset shows the optical rotation (mdeg) of SDS−RF complex at 330 nm with increasing temperatures. (b) Optical rotation (mdeg) of 20×10^{-3} M SDS−RF complex with increasing temperatures. Inset shows the optical rotation (mdeg) of SDS−RF complex at 330 nm with increasing temperatures.

evident from the figure that upon addition of SDS, it occupies the free space available in the system and thus increases the conductivity. When the concentration of SDS is high (CMC and above), it favors self-association of SDS molecules to form micelle. CMC is determined by the intersection of the two straight lines of the conductivity−concentration plots[22] and is found to be 5 mM in our experimental condition rather than 8 mM, which is the expected value of CMC for SDS in water. It
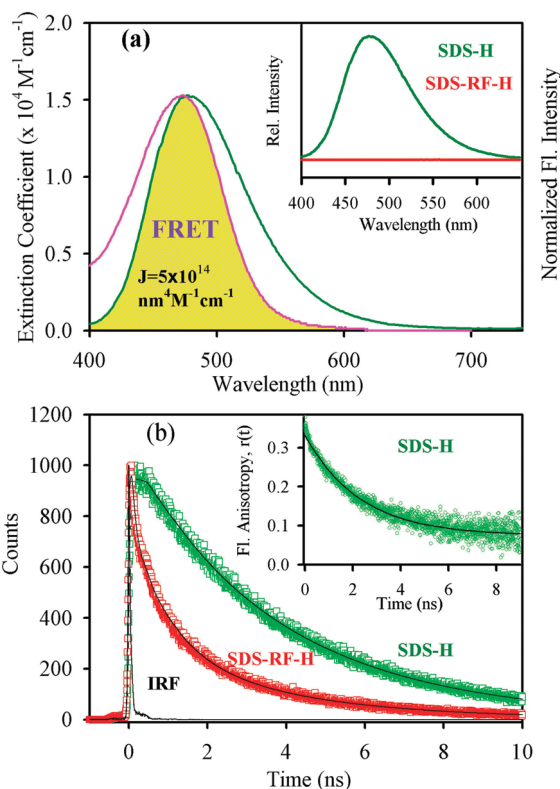

Figure 5. (a) Steady state absorption spectra of Rifampicin (RF; violet) and emission spectra of H33258−SDS (SDS−H; green) are shown. An overlapping zone between emission of H33258 and absorption of acceptor RF is indicated as yellow shaded zone. Inset shows the steady-state emission of SDS−H33258 (SDS−H) and SDS−RF−H33258 complex (SDS−RF−H). (b) The picosecond resolved fluorescence transients of SDS−H33258 (SDS−H) in absence (green) and in presence (red) of acceptor RF. Inset shows the fluorescence anisotropy, $r(t)$ of SDS−H33258 (SDS−H) complex. Excitation wavelength is 375 nm and data collected at 475 nm wavelength.

could be due to the presence of electrolytes, which causes a decrease in the CMC value of the ionic surfactant.[31] Figure 2b shows the variation of conductivity of SDS/RF/buffer ternary system. In Figure 2b, some significant change in the point of intersection of two lines (from 5 to 8 mM) is observed, where RF concentration is kept constant (0.2 mM) and the SDS concentration is varied. The break point (CMC of SDS) in presence of RF is shifted to relatively higher SDS concentration (8 mM). In an earlier study, on the complexation of β-cyclodextrin with the drug RF, similar conductometric patterns have been reported to confirm the binding of the drug with the cyclodextrin molecules.[22] The temperature-dependent conductivity of SDS/buffer and SDS/RF/buffer system has also been performed; however, no significant change in the slope of the conductivity−concentration plot is evident (results not shown).

RF has a remarkable CD characteristic[32] that makes the CD spectroscopy a suitable tool to study the effect of RF-binding to the SDS molecules. CD studies have been done on RF and SDS−RF complex in phosphate buffer at pH 7. On complexation with SDS, RF shows a change in CD band intensity as depicted in Figure 3. The inset of Figure 3 shows the absorption spectra of RF that does not alter significantly upon addition of SDS. The UV−vis spectroscopy is unable to provide any information of the interaction of RF with SDS, as shown in the inset of Figure 3. The
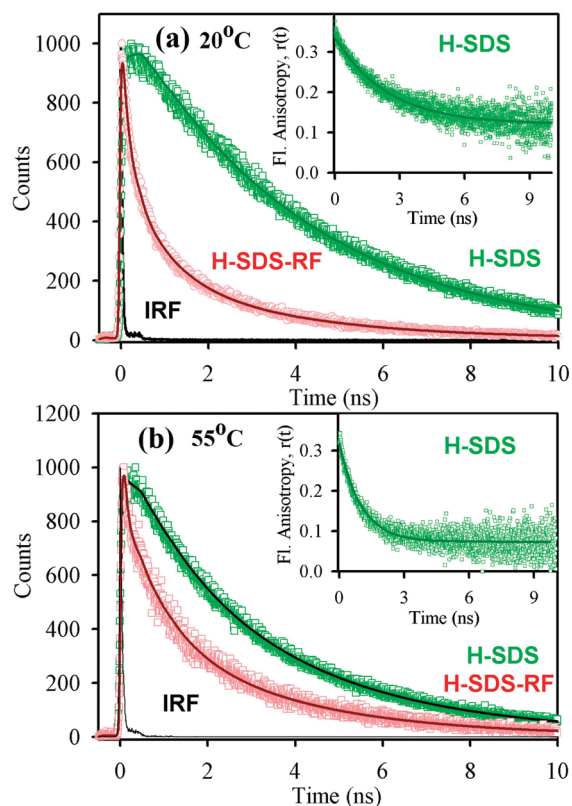
Figure 6. The picosecond-resolved fluorescence transients of H–SDS (H33258–SDS) in absence (green) and in presence (red) of acceptor RF (excitation at 375 nm) at (a) 20 °C. Inset shows the fluorescence anisotropy, $r(t)$ of H–SDS complex at 20 °C; (b) 55 °C. Inset shows the fluorescence anisotropy, $r(t)$ of H–SDS complex at 55 °C.

Table 1. Temperature-Dependent Fluorescence Lifetimes (τ_i) and Their Respective Amplitudes (amp %), Rotational Time Constant [τ_{rot}], Förster Resonance Energy Transfer (FRET) Efficiency (E), and FRET Distance (r) of H33258 (H–SDS) in SDS Micelle and H33258 (H–SDS–RF) in SDS Micelle–Rifampicin (RF) Complex[a]

systems	temp (°C)	τ_i (ns) (amp %)	τ_{av} (ns)	[τ_{rot}] (ns)	E (%)	r (Å)
H–SDS	20	4.1 (81%)	3.8	2.4		
		0.05 (19%)				
H–SDS–RF	20	3.3 (16%)	0.8		76	33
		0.91 (29%)				
		0.16 (55%)				
H–SDS	25	4.0 (84%)	3.5	2.3		
		1.6 (12%)				
		0.17 (4%)				
H–SDS–RF	25	3.5 (19%)	0.9		72	34
		0.93 (30%)				
		0.10 (51%)				
H–SDS	45	3.9 (65%)	2.9	1.2		
		1.61 (23%)				
		0.08 (12%)				
H–SDS–RF	45	3.4 (21%)	1		65	36
		0.87 (28%)				
		0.09 (51%)				
H–SDS	55	3.8 (61%)	2.8	1		
		1.59 (29%)				
		0.08 (10%)				
H–SDS–RF	55	3.2 (26%)	1.1		60	37
		0.85 (28%)				
		0.08 (46%)				

[a] The systems are excited at 375 nm and decay collected at 475 nm.

effect of temperature on the binding of RF to the SDS surfactant, near and far above the critical micellar concentrations, is examined by the temperature-dependent CD measurements and is depicted in Figure 4a,b, respectively. The CD spectra of the SDS–RF complex taken at different temperatures are analyzed to determine the change in ellipticity of the drug bound to the micelle. It is observed that the negative ellipticity of SDS–RF complex at 330 nm decreases with increasing the temperature from 20 to 90 °C for both the cases (near and far above the CMC). The nature of the slopes of the CD plots as shown in the insets of Figure 4a,b are similar. The observation clearly indicates that RF detaches from the micelle at higher temperature and it is independent of SDS concentration.

To confirm the binding of RF to the SDS micelle, another fluorescent dye H33258, bound to the SDS micelle, has been utilized. The emission spectrum of the dye H33258 in buffer shows a peak at 505 nm, which becomes blue shifted in hydrophobic environment (475 nm in SDS micelles),[26] as shown in Figure 5a. The binding of the donor drug H33258 to the micelle is confirmed by time-resolved anisotropy study. The fluorescence anisotropy, $r(t)$ (eq 5), which can decay in time due to the rotational motion of the molecules and consequently leads to depolarization of the fluorescence can be fitted to single exponential decay function to determine the rotational time constant (τ_{rot}) of the probe molecule (H33258).[25] The τ_{rot} value is found to be 2.3 ns (inset of Figure 5b) when bound to the micelle and 0.53 ns only in buffer, which is consistent with the values reported earlier.[26] The absorption spectrum of RF broadly

overlaps with the emission of H33258 bound to the SDS micelle (Figure 5a). The decrease in steady-state and time-resolved emission of H33258, bound to the micellar system, upon addition of RF is shown in the inset of Figure 5a,b, respectively. The efficiency of energy transfer is calculated by using eq 4b and found to be 72%. The estimated Förster distance (R_0), utilizing eq 1, and donor (H33258)–acceptor (RF) distance (r) are found to be 40 and 34 Å, respectively (at 25 °C). The observation indicates simultaneous binding of the two drugs to the micelle at room temperature.

To study the thermal stability of the drug binding to the SDS micelle, we have performed picosecond-resolved temperature dependent FRET experiments, as shown in Figure 6. From the temperature dependent fluorescence anisotropy of the donor H33258 bound to the micelle it is evident that the dynamics of anisotropy becomes faster with increasing temperature. The rotational relaxation time (τ_{rot}) of the probe is related to the local microviscosity (η_m) of the probe environment according to the Stokes–Einstein–Debye equation (SED) as

$$\tau_{rot} = \frac{\eta_m V_h}{k_B T} \qquad (6)$$

where k_B is the Boltzmann constant, T is the absolute temperature, and V_h is the hydrodynamic volume of the probe. It is very clear from this equation and the earlier report that the value of rotational time constant (τ_{rot}) is supposed to decrease with increasing temperature.[33] This is due to the increased thermal
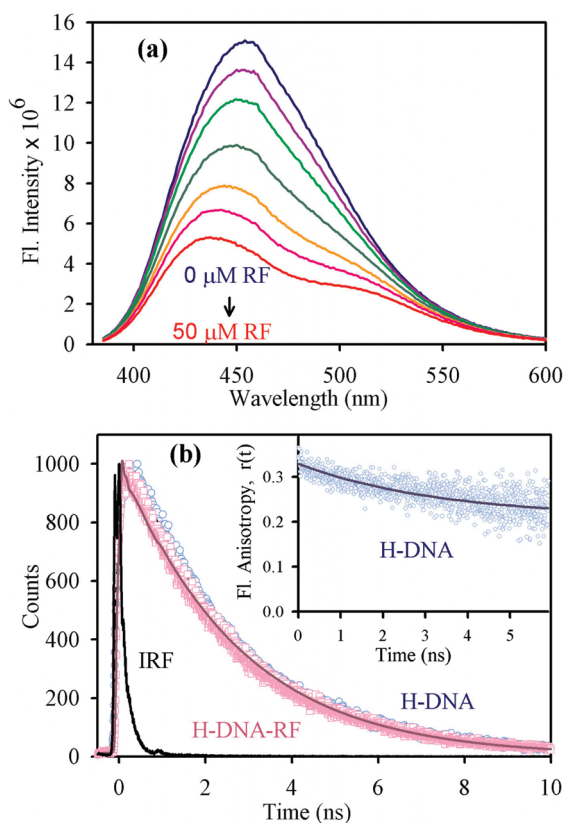
Figure 7. (a) Steady-state fluorescence spectra of DNA-bound H33258 (H−DNA) with increasing concentration of RF. (b) The picosecond-resolved fluorescence transients of H33258−DNA in absence (blue) and in presence (pink) of acceptor RF (H−DNA−RF) (excited at 375 nm and decay collected at 450 nm). Inset shows the fluorescence anisotropy, $r(t)$ of H33258−DNA complex.

motion of the surfactant molecules with increasing temperature, which in turn causes a decrease in the microviscosity of the environment experienced by the probe (H33258) in the micellar solution. Decrease in energy transfer efficiency and increase in donor (H33258)−acceptor (RF) distance with increasing temperature is evident from Table 1. An attempt to fit the fluorescence transients using biexponential functions also reveals reasonable good fitting yielding similar donor−acceptor distances; however, energy transfer efficiencies are found to be 71% (at 20 °C) and 43% (at 55 °C).

It is known that RF is a specific inhibitor of bacterial RNA polymerase and inhibits the process of transcription at the level of initiation.[13−16] It is also known that RF forms a 1:1 complex with RNA polymerase.[34] However, the possibility of direct interaction of the drug with DNA is not investigated until now. To study the interaction of DNA with RF we have used the fluorescence of synthesized dodecamer-bound minor groove binder, drug H33258[35] in RF solution. Figure 7a shows the steady-state emission of the DNA-bound H33258 in presence of varying concentrations of RF and in absence of RF as well. It is clear from Figure 7a that H33258−DNA fluorescence is significantly decreased upon increasing the concentration of RF in the solution and additionally a hump at 505 nm (similar to the fluorescence peak in bulk water) is observed at higher concentrations of RF. The observation is consistent with the fact that a small amount of H33258 is being detached from DNA in the

presence of RF. In the Figure 7b, the fluorescence transients of H33258 in the dodecamer DNA without and with RF are shown. The slower rotational depolarization decay in the inset of Figure 7b indicates the attachment of the drug H33258 to the DNA minor groove. Insignificant change in the fluorescence lifetime of the probe H33258 bound to DNA in the presence of RF clearly rules out the possibility of any direct interaction of RF with the DNA. To reconfirm the competitive nature of the DNA binding of RF, CD spectroscopy has also been utilized. However, the CD spectrum of dodecamer DNA or RF upon mixing shows insignificant change compared to spectrum of the DNA and RF in bulk buffer. Thus, it is evident from the CD spectroscopy data that RF probably does not have any direct interaction with the DNA. Although a firm conclusion of the detachment of H33258 and lack of direct interaction of RF with the DNA invites more experiments, one of the possible causes could be significant alteration in the nature of DNA hydration in presence of RF in the solution.[36]

■ CONCLUSION

In this report we have explored the binding of an antituberculosis drug RF to a model anionic SDS micelle. We have utilized dynamic light scattering and conductometric studies to characterize the structural changes of the SDS micelle upon binding of RF. Additionally, circular dichroism spectroscopy has been employed to characterize the binding of the drug to the micelle. The temperature-dependent studies on the drug micelle complex reveal the partial detachment of the drug from the micelle at elevated temperature and also that the structural integrity of the complex is maintained throughout the range of temperature studied. The strong absorption band in the visible region of the drug RF has been employed to monitor resonance energy transfer from an antihelminthic fluorescent drug H33258 at the micellar surface. Förster resonance energy transfer confirms the simultaneous binding of the two drugs to the micelle. The study at various temperatures confirms that the location and efficiency of drug binding to the micelle change significantly. Steady-state and time-resolved studies on a synthesized DNA-bound H33258 in RF solution indicate that H33258 detaches from the DNA upon addition of RF and CD studies rules out the interaction of DNA with the drug RF. Our spectroscopic studies are expected to find their relevance in the exploration of interaction of the important hydrophobic drug RF with other macromolecular assemblies for the discovery of better drug-vehicle for the sparingly aqueous soluble drug RF.

■ AUTHOR INFORMATION

Corresponding Author
*E-mail: skpal@bose.res.in, spal@caltech.edu.

Present Addresses
[†]Arthur Amos Noyes Laboratory of Chemical Physics, California Institute of Technology (CALTECH), 1200 East California Boulevard, Pasadena, CA 91125, United States.

■ REFERENCES

(1) Cohen, T.; Lipsitch, M.; Walensky, R. P.; Murray, M. *Proc. Natl. Acad. Sci. U.S.A.* **2006**, *103*, 7042.

(2) Medoff, G.; Kobayashi, G. S.; Kwan, C. N.; Schlessinger, D.; Venkov, P. *Proc. Natl. Acad. Sci. U.S.A.* **1972**, *69*, 196.

(3) Zhang, Y.; Dhandayuthapani, Y.; Deretic, V. *Proc. Natl. Acad. Sci. U.S.A* **1996**, *93*, 13212.

(4) Ge, F.; Zeng, F.; Liu, S. *J. Med. Microbiol.* **2010**, *59*, 567.

(5) Dye, C.; Williams, B. G. *Proc. Natl. Acad. Sci. U.S.A.* **2000**, *97*, 8180.

(6) Dickinson, J. M.; Aber, V. R.; Mitchison, D. A. *Am. Rev. Respir. Dis.* **1977**, *116*, 627.

(7) Borba, A.; Gmez-Zavaglia, A.; Fausto, R. *J. Phys. Chem. A* **2009**, *113*, 9220.

(8) Alteri, C. J.; Cortes, J. X.; Hess, S.; Olín, G. C.; Girón, J. A.; Friedman, R. L. *Proc. Natl. Acad. Sci. U.S.A.* **2007**, *104*, 5145.

(9) Rodrigues, C.; Gameiro, P.; Prieto, M.; Castro, B. *Biochim. Biophys. Acta* **2003**, *1620*, 151.

(10) Moraski, G. C.; Chang, M.; Villegas-Estrada, A. *Eur. J. Med. Chem.* **2010**, *45*, 1703.

(11) Cavicchioli, M.; Massabni, A. C.; Heinrich, T. A. *J. Inorg. Biochem.* **2010**, *104*, 533.

(12) Luciani, F.; Sisson, S. A.; Jiang, H.; Francis, A. R.; Tanaka, M. M. *Proc. Natl. Acad. Sci. U.S.A.* **2009**, *106*, 14711.

(13) Bahr, W.; Stender, W.; Scheit, K. H.; Jovin, T. M. *RNA polymerase*; Cold Spring Harbor: New York, 1976.

(14) So, A. G.; Downey, K. M. *Biochemistry* **1970**, *9*, 4788.

(15) Johnston, D. E.; McClure, W. R. *RNA polymerase*; Cold Spring Harbor: New York, 1976.

(16) Campbell, E. A.; Korzheva, N.; Mustaev, A.; Murakami, K.; Nair, S.; Goldfarb, A.; Darst, S. A. *Cell* **2001**, *104*, 901.

(17) Langer, R. *Science* **2001**, *293*, 58.

(18) Huwyler, J.; Wu, D.; Pardridge, W. M. *Proc. Natl. Acad. Sci. U.S.A.* **1996**, *93*, 14164.

(19) Hubbell, J. A. *Science* **2003**, *300*, 595.

(20) Hillmyer, M. A. *Science* **2007**, *317*, 604.

(21) Sullivan, S. M.; Huang, L. *Proc. Natl. Acad. Sci. U.S.A.* **1986**, *83*, 6117.

(22) Mehta, S. K.; Bhasin, K. K.; Mehta, N.; Dham, S. *Colloid Polym. Sci.* **2005**, *283*, 532.

(23) Mall, S.; Buckton, G.; Rawlins, D. A. *J. Pharm. Sci.* **1996**, *85*, 75.

(24) Chen, H.; Kim, S.; Li, L.; Wang, S.; Park, K.; Cheng, J. X. *Proc. Natl. Acad. Sci. U.S.A.* **2008**, *105*, 6596.

(25) Lakowicz, J. R. *Principles of Flourescence Spectroscopy*, 2nd ed; Kluwer Academic/Plenum Publishers: New York, 1999.

(26) Banerjee, D.; Pal, S. K. *Chem. Phys. Lett.* **2006**, *432*, 257.

(27) Majumder, P.; Sarkar, R.; Shaw, A. K.; Chakraborty, A.; Pal, S. K. *J. Colloid Interface Sci.* **2005**, *290*, 462.

(28) O'Connor, D. V.; Phillips, D. *Time-Correlated Single Photon Counting*; Academic Press: London, 1984.

(29) Mitra, R. K.; Sinha, S. S.; Pal, S. K. *J. Phys. Chem. B* **2007**, *111*, 7577.

(30) Howes, B. D.; Guerrini, L.; Sanchez-Cortes, S.; Marzocchi, M. P.; Garcia-Ramos, J. V.; Smulevich, G. *J. Raman Spectrosc.* **2007**, *38*, 859.

(31) Fuguet, E.; Ràfols, C.; Rośes, M.; Bosch, E. *Anal. Chim. Acta* **2005**, *548*, 95.

(32) Reisbig, R. R.; Woody, A. Y. M.; Woody, R. W. *Biochemistry* **1982**, *21*, 196.

(33) Verma, P. K.; Mitra, R. K.; Pal, S. K. *Langmuir* **2009**, *25*, 11336.

(34) Kumar, K. P.; Reddy, P. S.; Chatterji, D. *Biochemistry* **1992**, *31*, 7519.

(35) Pal, S. K.; Zhao, L.; Zewail, A. H. *Proc. Natl. Acad. Sci. U.S.A.* **2003**, *100*, 8113.

(36) Yonetani, Y.; Kono, H. *Biophys. J.* **2009**, *97*, 1138.